Molecular Crystals and Liquid Crystals
Publication details, including instructions for authors and subscription information:
http://www.tandfonline.com/loi/gmcl20

Ultra Simple Fluorescent White Organic Light-Emitting Diodes Using Fluorescent Green-Yellow Emitter and Blue Host

Ji Hoon Seo [a], Jung Sun Park [a], Jun Ho Kim [a], Kum Hee Lee [b], Jung Yeon Kim [b], Seung Soo Yoon [b] & Young Kwan Kim [a]

[a] Department of Information Display, Hongik University, Seoul, Korea
[b] Department of Chemistry, Sungkyunkwan University, Suwon, Korea

Version of record first published: 19 Apr 2010

To cite this article: Ji Hoon Seo, Jung Sun Park, Jun Ho Kim, Kum Hee Lee, Jung Yeon Kim, Seung Soo Yoon & Young Kwan Kim (2010): Ultra Simple Fluorescent White Organic Light-Emitting Diodes Using Fluorescent Green-Yellow Emitter and Blue Host, Molecular Crystals and Liquid Crystals, 520:1, 83/[359]-89/[365]

To link to this article: http://dx.doi.org/10.1080/15421401003609756

Mol. Cryst. Liq. Cryst., Vol. 520: pp. 83/[359]–89/[365], 2010

ISSN: 1542-1406 print/1563-5287 online
DOI: 10.1080/15421401003609756

Taylor & Francis
Taylor & Francis Group

Ultra Simple Fluorescent White Organic Light-Emitting Diodes Using Fluorescent Green-Yellow Emitter and Blue Host

JI HOON SEO,[1] JUNG SUN PARK,[1] JUN HO KIM,[1]
KUM HEE LEE,[2] JUNG YEON KIM,[2]
SEUNG SOO YOON,[2] AND YOUNG KWAN KIM[1]

[1]Department of Information Display, Hongik University, Seoul, Korea
[2]Department of Chemistry, Sungkyunkwan University, Suwon, Korea

The authors have demonstrated ultra simple fluorescent white organic light-emitting diodes using fluorescent green-yellow emitter of 9,10-bis[4-(di-4-tert-butylphenylamino) styryl]anthracene and blue host of 2-methyl-9,10-di(2-naphthyl)anthracene. The optimized device at the extremely low doping concentration (0.2 wt.%) of green-yellow emitter showed a luminous efficiency of 7.18 cd/A, a power efficiency of 5.64 lm/W at 100 cd/m^2, and a Commission Internationale de I'Eclairage coordinates of (0.35, 0.43) at 6 V, respectively.

Keywords The extremely low doping concentration; ultra simple fluorescent white organic light-emitting diodes

Introduction

Organic light-emitting diodes (OLEDs) have attracted increasing attention for next generation flat panel displays due to mechanical flexibility, thinness, wide-viewing angle, low-voltage operation, high resolution, and a fast response time [1–4].

One of the most important keys for OLEDs is high efficiency. An efficiency of OLEDs also have been improved gradually for two decades after C. W. Tang *et al.* have published a paper on bi-layered structure of OLED [1]. The device structures for high efficiency have been intensively studied by various methods such as multi-emitting layer (EML) system [5], co-host system [6], the introduction of spacer [7], p-i-n, [8], microcavity, [9], and tandem structure [10]. However, these methods have some drawbacks such as complicated process, high production cost, and long tact-time. Recently, a few researches have been reported for overcoming those drawbacks [11,12]. We have also published some experimental results for ultra simple blue OLEDs in elsewhere [13].

White organic light-emitting diodes (WOLEDs) have drawn increasing attention due to their potential use in various applications such as solid-state lighting and

Address correspondence to Young Kwan Kim, Department of Information Display, Hongik University, Sangsu-dong, Mapo-ku, Seoul 121-797, Korea (ROK). Tel.: (+82)2-3142-3750; Fax: (+82)2-3142-0335; E-mail: kimyk@hongik.ac.kr

backlight of liquid crystal displays (LCDs) and full-color OLEDs of red, green, and blue pixels. A variety of methods have been suggested for the WOLEDs fabrications. WOLEDs are generally fabricated with all fluorescent and phosphorescent layers [14,15], hybrid EML [16], micro-cavity [17], blue EML with down conversion layer [18], and tandem stuructures [19]. However, these WOLEDs were demonstrated by complicated process with more than five organic materials generally. Simple WOLEDs for potential candidate for general lighting applications would be of significant advantage such as a low cost and short process for low-end and low-cost general lighting applications [20].

In this paper, we report ultra simple fluorescent WOLEDs using only fluorescent green-yellow emitter of 9,10-bis[4-(di-4-tert-butylphenylamino)styryl]anthracene (ATBTPA) and blue host of 2-methyl-9,10-di(2-naphthyl)anthracene (MADN). WOLEDs exhibited the maximum luminous efficiency of 7.12 cd/A at 5.76 mA/cm^2, the maximum power efficiency of 5.35 lm/W at 1.55 mA/cm^2, and Commission Internationale de I'Eclairage ($CIE_{x,y}$) of (0.38, 0.47) at 6 V, respectively.

Experimental

Fabrication of OLED

Indium tin oxide (ITO)-coated glass was cleaned in an ultrasonic bath by the following sequence: in acetone, methanol, distilled water and isopropyl alcohol. Thereafter, pre-cleaned ITO was treated by O_2 plasma with the conditions of 2×10^{-2} Torr, 125 W for 2 min. WOLEDs were fabricated using the high vacuum (5×10^{-7} Torr) thermal evaporation of organic materials onto the surface of the ITO-coated glass substrate (30 Ω/sq, emitting area was 3 mm × 3 mm). The deposition rates were 1.0∼1.1 Å/sec for MADN and 4,7-diphenyl-1,10-phenanthroline (BPhen) and 0.1 Å/sec for lithium quinolate (Liq), respectively. Without a vacuum break after the deposition of organic layers, the aluminum (Al) cathode was deposited at a rate of 10 Å/sec. The ultra violet (UV)/visible absorption and photoluminescence (PL) spectra were measured with LS-55.

Measurements

With the DC voltage bias, the optical and electrical properties of WOLEDs such as the current density, luminance, luminous efficiency, power efficiency, and electroluminescence (EL) spectra of the emission characteristics were measured with Keithley 2400 and CHROMA METER CS-1000A instruments. The $CIE_{x,y}$ coordinates were also calculated with Keithley 2400 and CHROMA METER CS-1000A instruments. All measurements were carried out under ambient conditions at room temperature.

Results and Discussion

Figure 1 (a) shows the molecular structure of key materials used for fabrication, MADN, ATBTPA, and BPhen, respectively. The energy level diagram of the device is also shown in Figure 1 (b), where all device A, B, C, D, E, and F have the structure of ITO (1500 Å)/MADN (600 Å)/MADN:ATBTPA (x%, 300 Å)/BPhen (200 Å)/Liq (20 Å)/Al (1000 Å) with the doping concentration of ABTAPA was 0, 0.1, 0.2, 0.3, 0.5, and 1 wt.%, respectively. Here, MADN, ATBTPA, BPhen, and Liq were

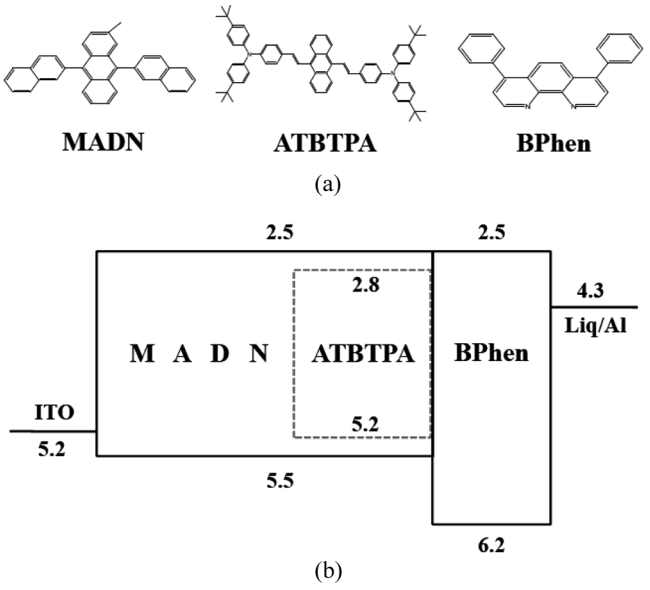

Figure 1. (a) Molecular structure of the key materials, MADN, ATBTPA, and BPhen, used for fabrication. (b) Energy level diagrams for white organic light-emitting diodes (WOLEDs). Numbers showed the highest occupied molecular orbital (HOMO) and lowest unoccupied molecular orbital (LUMO) of various materials used in this study.

used as blue host, green-yellow emitter, hole blocking layer, and electron injection layer, respectively. BPhen having high electron mobility of $10^{-4}\,cm^2/V\,s$ was used for the optimized recombination zone because devices had smaller hole-injection barrier of 0.3 eV between highest occupied molecular orbital (HOMO) of ITO and that of MADN than electron-injection barrier of 1.8 eV between lowest unoccupied molecular orbital (LUMO) of Liq/Al and that of MADN. Here, MADN had lower electron mobility of $10^{-4}\,cm^2/V\,s$ than that of BPhen.

Figure 2 shows the UV/visible absorption and PL spectra of ATBTPA and MADN, respectively. The maximum UV/visible absorption peak of ATBTPA was 427 nm and the maximum PL peak of MADN was 434 nm, respectively. The UV/visible absorption of ATBTPA and PL spectra of MADN showed a good spectral overlap which could explain an efficient Förster singlet energy transfer from MADN to ATBTPA. Therefore, in order to have white emission with the fluorescent emitter of ATBTPA and the host of MADN, it is necessary to minimize the energy transfer from MADN to ATBTPA by using the extremely low doping concentration of ATBTPA.

Figure 3 shows the current density versus voltage characteristics of all devices fabricated in this study, where all devices except device A were doped with ATBTPA at the concentration of 0.1, 0.2, 0.3, 0.5, and 1 wt.%, respectively. They demonstrated the maximum current density of 85.38, 45.53, 44.69, 39.82, 38.75, and 37.61 mA/cm^2 at 8 V from device A to device F, respectively. All devices having dopant of ATBTPA had the lower current density than device A because doped devices showed poor hole and electron transport properties which seemed to be due to the trap site near by the HOMO of 5.2 eV and the LUMO of 2.8 eV. Therefore, the device F having the highest

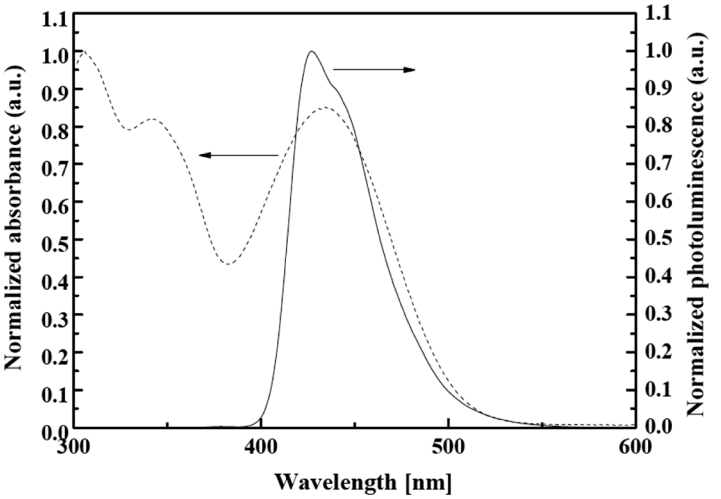

Figure 2. Normalized ultra violet (UV)/visible absorption of ATBTPA and normalized photoluminescence (PL) spectra of MADN.

doping concentration of ATBTPA showed the lowest current density among them at operating voltages.

Figure 4(a) and (b) shows the $CIE_{x,y}$ coordinates versus operating voltages from 4 to 8 V and EL spectra of all devices with various doping concentration of ATBTPA. All devices had an emission of $CIE_{x,y}$ coordinates from (0.15, 0.06), (0.25, 0.25), (0.39, 0.48), (0.40, 0.50), (0.42, 0.52), and (0.45, 0.52) at 4 V to (0.15,

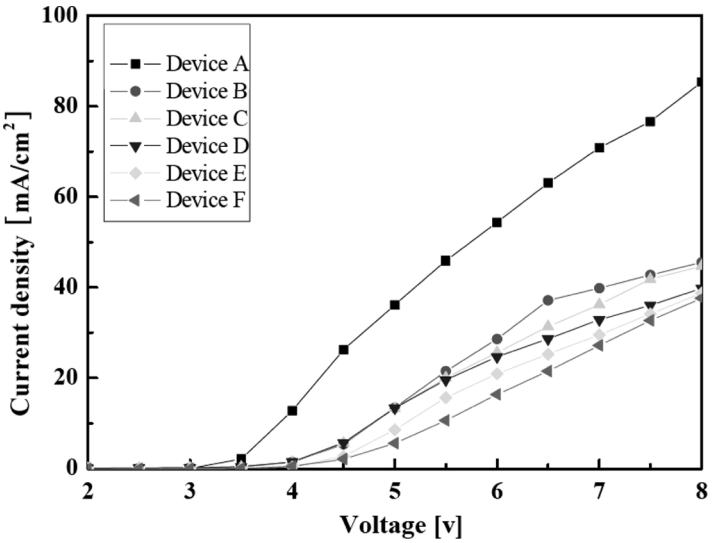

Figure 3. Current density (J) versus voltage (V) characteristivs of all devices, where all device A, B, C, D, E, and F have the structure of ITO (1500 Å)/MADN (600 Å)/MADN:ATBTPA (x%, 300 Å)/BPhen (200 Å)/Liq (20 Å)/Al (1000 Å) with the doping concentration of ABTAPA was 0, 0.1, 0.2, 0.3, 0.5, and 1 wt.%, respectively.

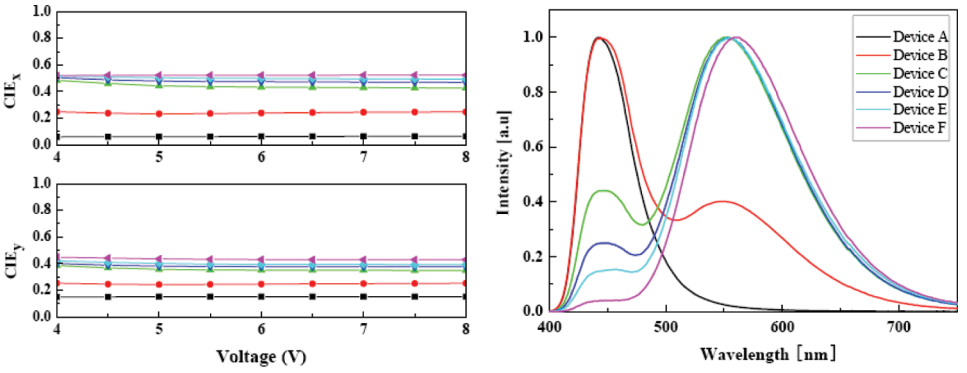

(a) (b)

Figure 4. (a) Commission Internationale de I'Eclairage ($CIE_{x,y}$) coordinates of all devices from 4 V to 8 V. (b) Electroluminescence (EL) spectra of all devices at 6 V.

0.06), (0.25, 0.25), (0.35, 0.43), (0.38, 0.47), (0.39, 0.49), and (0.43, 0.52) at 8 V, respectively. They had an emission of $CIE_{x,y}$ coordinates from ($x = 0.15$, $y = 0.06$), ($x = 0.25$, $y = 0.24$), ($x = 0.35$, $y = 0.43$), ($x = 0.38$, $y = 0.47$), ($x = 0.40$, $y = 0.50$), and ($x = 0.43$, $y = 0.52$) at 6 V, respectively. All spectra were measured at a constant voltage of 6 V as shown in Figure 4(b). Device B showed cold white emission and, on the other hand, device C and D showed warm white emission. Device B showed smaller color shift with $\Delta CIE_{x,y}$ of $\pm(0.00, 0.01)$ from 4 to 8 V in Figure 4(a). It was also shown in Figure 4(b) that all devices had blue peak of MADN from 442 to 447 nm and green-yellow peak of ATBTPA from 550 to 560 nm, where the blue peak intensity from MADN tends to decrease as the doping concentration of ATBTPA increases. Device A showed only MADN peak of 420 nm and, on the other hand, device F with doping concentration of 1% mostly showed ATBTPA peak of 560 nm, which indicates an efficient Föster singlet energy transfer from MADN to ATBTPA. Device B giving cold white emission showed 1:0.4 ratio of blue to

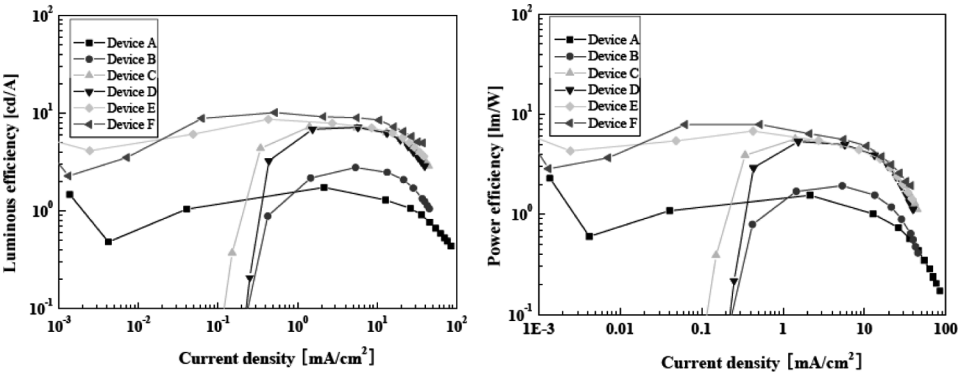

(a) (b)

Figure 5. (a) Luminous efficiency (LE) versus current density (J) characteristics of all devices. (b) Power efficiency (PE) versus current density (J) characteristics of all devices.

Table 1. Various characteristics of WOLED device B, C, and D, including luminance at 4 V, max. luminous efficiency, max. external efficiency, and $CIE_{x,y}$ coordinates at 6 V

Device	Luminance [cd/m^2] at 4 V	Max. luminous efficiency [cd/A]	Max. Power efficiency [lm/W]	$CIE_{x,y}$ at 6 V
B	32	2.76	1.92	0.25, 0.24
C	102	7.18	5.64	0.35, 0.43
D	105	7.12	5.35	0.38, 0.47

green-yellow peak and device C and D giving warm white emission showed 0.4:1 and 0.2:1 ratio, respectively.

Figure 5(a) and (b) show the luminous efficiency and power efficiency versus current density for all devices, where device A, B, C, D, E, and F had the maximum luminous efficiency of 1.73, 2.76, 7.18, 7.12, 8.61, and 10.01 cd/A at 2.15, 5.37, 1.42, 5.76, 0.43, and 0.52 mA/cm^2, and the maximum power efficiency of 1.55, 1.92, 5.64, 5.35, 6.76, and 7.90 lm/W at 2.15, 5.37, 1.42, 1.55, 0.43, and 0.52 mA/cm^2, respectively. Device F showed the highest luminous and power efficiency among them because device F with doping concentration of 1% showed the most efficient Föster singlet energy transfer. The luminous efficiency of 7.12 cd/A with this simple WOLEDs is one of the highest among the others reported for any WOLEDs based on one green-yellow fluorescent emitter without HTL such as N,N′-Bis(3-methylphenyl)-N,N′-bis(phenyl)-benzidine and N,N′-Bis(naphthalen-1-yl)-N,N′-bis(phenyl)-benzidine.

The various characteristics of white device B, C, and D were summarized in Table 1, such as luminance at 4 V, maximum luminous efficiency, maximum power efficiency, and $CIE_{x,y}$ coordinates at 6 V, respectively.

Conclusions

We demonstrated in this letter that ultra simple WOLEDs using one fluorescent green-yellow emitter of ATBTPA and blue host of MADN. The simple white device exhibited a luminous efficiency of 7.18 cd/A, a power efficiency of 5.64 lm/W at 100 cd/m^2, and a $CIE_{x,y}$ coordinates of (0.35, 0.43) at 6 V, respectively. This result is among the best reported for any WOLEDs based on one red fluorescent emitter without HTL. This simple WOLEDs would be of advantage such as a low cost and simple fabrication process for low-end and low-cost general lighting applications.

Acknowledgment

This work was supported by the ERC program of the Korea Science and Engineering Foundation (KOSEF) grant funded by the Korea Ministry of Education, Science and Technology (MEST) (No. R11-2007-045-03001-0).

References

[1] Tang, C. W. & VanSlyke, S. A. (1987). *Appl. Phys. Lett.*, *51*, 913.
[2] Kido, J., Hongawa, K., Okuyama, K., & Nagai, K. (1994). *Appl. Phys. Lett.*, *64*, 815.

[3] Zhang, H. M. & Choy, W. C. H. (2008). *Organic Electrons*, *9*, 964.
[4] Chopra, N., Lee, J. W., Zheng, Y., Eom, S. H., Xue, J., & So, F. (2008). *Appl. Phys. Lett.*, *93*, 143307.
[5] Kang, J. W., Lee, S. H., Park, H. D., Jeong, W. I., Yoo, K. M., Park, Y. S., & Kim, J. J. (2007). *Appl. Phys. Lett.*, *90*, 223508.
[6] Kim, S. H., Jang, J. S., & Lee, J. Y. (2007). *Appl. Phys. Lett.*, *91*, 083511.
[7] Yang, D., Li, W., Chu, B., Zhang, D., Zhu, J., Su, Z., Su, W., Han, L., Bi, D., Chen, Y., Yan, F., Liu, H., & Wang, D. (2008). *Appl. Phys. Lett.*, *92*, 253309.
[8] Huang, J., Pfeiffer, M., Werner, A., Blochwitz, J., Leo, K., & Liu, S. (2002). *Appl. Phys. Lett.*, *80*, 139.
[9] Lin, C. L., Lin, H. W., & Wu, C. C. (2005). *Appl. Phys. Lett.*, *87*, 021101.
[10] Liao, L. S. & Klubek, K. P. (2008). *Appl. Phys. Lett.*, *92*, 223311.
[11] Park, T. J., Jeon, W. S., Park, J. J., Kim, S. Y., Lee, Y. K., Jang, J., Kwon, J. H., & Pode, R. (2008). *Appl. Phys. Lett.*, *92*, 113308.
[12] Jeon, W. S., Park, T. J., Park, J. J., Kim, S. Y., Jang, J., Kwon, J. H., & Pode, R. (2008). *Appl. Phys. Lett.*, *92*, 113311.
[13] Seo, J. H., Kim, G. Y., Koo, J. R., Park, J. S., Seo, B. M., Lee, K. H., You, J. N., Yoon, S. S., & Kim, Y. K. Org. Electron. Contributing. A detailed ultra simple blue OLEDs will be reported elsewhere: G. Y. Kim, J. H. Seo, and Y. K. Kim, in preparation.
[14] Wang, Y., Hua, Y. L., Wu, X. M., Zhang, L. J., Hou, Q. C., & Liu, Q. (2008). *Organic Electronics*, *9*, 273.
[15] Su, S. J., Gonmori, E., Sasabe, H., & Kido, J. (2008). *Adv. Mater.*, *20*, 4189.
[16] Seo, J. H., Kim, J. H., Seo, J. H., Hyung, G. W., Park, J. H., Lee, K. H., Yoon, S. S., & Kim, Y. K. (2007). *Appl. Phys. Lett.*, *90*, 203507.
[17] Cao, J., Liu, X., Kahn, M. A., Zhu, W. Q., Jiang, X. Y., Zhang, Z. L., & Xu, S. H. (2007). *Current Applied Physics*, *7*, 300.
[18] Mazzeo, M., Pisignano, D., Favaretto, L., Sotgiu, G., Barbarella, G., Cingolani, R., & Gigli, G. (2003). *Synthetic Metals*, *139*, 675.
[19] Chang, C. C., Chen, J. F., Hwang, S. W., & Chen, C. H. (2005). *Appl. Phys. Lett.*, *87*, 253501.
[20] Anzenbacher, P., Jr., Montes, V. A., & Takizawa, S. Y. (2008). *Appl. Phys. Lett.*, *93*, 163302.